ENVIRONMENTAL RESEARCH
LETTERS

LETTER

Ammonia transfers through interprovincial agricultural trade and their health burden implications in China

Junjie Liu[1], **Baojie Li**[1,*], **Qing Zhu**[2,*], **Yongqi Zhao**[1], **Teng Wang**[3], **Kaihua Liao**[2], **Yan Li**[4], **Wanglijin Gu**[1], **Weimeng Zhang**[1] and **Hong Liao**[1,*]

[1] Collaborative Innovation Center of Atmospheric Environment and Equipment Technology, Jiangsu Key Laboratory of Atmospheric Environment Monitoring and Pollution Control, School of Environmental Science and Engineering, Nanjing University of Information Science and Technology, Nanjing 210044, People's Republic of China
[2] Key Laboratory of Watershed Geographic Sciences, Nanjing Institute of Geography and Limnology, Chinese Academy of Sciences, Nanjing 210008, People's Republic of China
[3] College of Oceanography, Hohai University, Nanjing 210024, People's Republic of China
[4] School of Urban Planning and Design, Peking University Shenzhen Graduate School, Shenzhen 518055, People's Republic of China
* Authors to whom any correspondence should be addressed.

E-mail: baojieli@nuist.edu.cn, qzhu@niglas.ac.cn and hongliao@nuist.edu.cn

Keywords: agricultural trade, NH_3 emission transfer, $PM_{2.5}$, premature mortality

Supplementary material for this article is available online

OPEN ACCESS

RECEIVED
8 May 2025

REVISED
24 June 2025

ACCEPTED FOR PUBLICATION
17 July 2025

PUBLISHED
25 July 2025

Abstract

The spatial mismatch between agricultural resources and market demand across China creates significant challenges for food security and environmental management. Although interprovincial agricultural trade can alleviate regional food supply pressures, substantial uncertainties persist regarding the associated ammonia (NH_3) emission transfers and their impacts on air quality and human health. Here we fill this gap using a linear programming model to simulate interprovincial trade flows of 26 individual agricultural products, combined with high-resolution NH_3 emission inventories and air quality simulation. We found that interprovincial trade-related NH_3 emissions reached 2.94 Tg in 2019, accounting for 28.1% of total agricultural NH_3 emission, with predominant transfers from eastern and southern China to northern and central China. These trade-related NH_3 emissions contributed 2.6 $\mu g\ m^{-3}$ to annual $PM_{2.5}$ concentrations and caused 252 016 associated premature deaths. Mortality response to trade-related NH_3 emissions exhibited spatial heterogeneity across China, driven by regional variations in population density and $PM_{2.5}$ sensitivity to NH_3 emissions. Agricultural trade generated disproportionate health impacts, with Central China, Southwest China, North China, and Northeast China collectively receiving a net inflow of 28 776 premature deaths. Our results demonstrate that a cross-provincial ecological compensation mechanism needs to be established to balance agricultural trade's impact on food security, air quality, and human health.

1. Introduction

Agricultural trade plays a crucial role in addressing the spatial mismatch between production and demand across regions, particularly in countries with heterogeneous resource distribution like China (Feng *et al* 2013, Wei *et al* 2020). While agricultural trade is essential for food security, it also results in the transfer of environmental impacts across regions. With food system responsible for more than 80% of total ammonia (NH_3) emissions (Huang *et al* 2012), significant trade-driven transfers of NH_3 emissions occur from importing to exporting regions. As a major alkaline gas, NH_3 facilitates the formation of secondary inorganic aerosols, thereby increasing the concentration of $PM_{2.5}$ and associated premature mortality (Burnett *et al* 2014, Xie *et al* 2016, Fu *et al* 2017, Geng *et al* 2021), which indicates that agricultural trade can reshape the spatial patterns of $PM_{2.5}$ pollution and redistribute health burdens through the transfer of NH_3 emissions. The combination of substantial reductions in acidic gas emissions and critically

insufficient NH_3 emission controls has elevated NH_3 emission as a dominant driver of $PM_{2.5}$ pollution in China (Wang *et al* 2011, Bai *et al* 2019, Liu *et al* 2019, Gu *et al* 2021, Guo *et al* 2024). Reducing agricultural NH_3 volatilization while satisfying the food demand is strategically required to mitigate haze pollution (Zhan *et al* 2020).

To date, China has implemented policies to control agricultural NH_3 emissions, such as the 14th Five-Year Plan's proposed 5% reduction in NH_3 emissions from large-scale livestock farms in heavily polluted regions, implementation of family farm development programs, and Zero Growth of Chemical Fertilizers Plan (Li *et al* 2024). However, these policies primarily control NH_3 emissions and improve air quality from a nitrogen management perspective, with limited consideration of trade-related aspects. In 2018, a revised cropland protection policy was introduced in China to allow cross-provincial cropland displacement, potentially increasing agricultural trade and embodied NH_3 emission transfers (Yang *et al* 2020). Consequently, managing agricultural trade-related NH_3 emissions is critical for both food security and sustained air quality improvement. Here, the 'trade-related NH_3 emissions' for a given province refers to the NH_3 emissions generated by that province during the production of agricultural products exported to other provinces, specifically emissions from fertilizer application and livestock waste.

NH_3 emission transfers through the global trade network can be quantified by global multi-regional input–output (MRIO) models, which have been applied to measure resource and greenhouse gas transfers embodied in agricultural trade at both global and national scale (Yang *et al* 2012, Qiang *et al* 2013, Zhuo *et al* 2016, Ali *et al* 2017, Liu *et al* 2018, 2021, 2023, Wu *et al* 2018, Wang *et al* 2019b, Chen *et al* 2022, Zhang *et al* 2023, Ju *et al* 2024, Pan *et al* 2024). Ma *et al* explored the mitigation potential of global ammonia emissions by analyzing the role of the international trade network (Ma *et al* 2021). Nevertheless, how agricultural trade restructures regional NH_3 emissions and their environmental impacts in China remains poorly quantified, particularly at the provincial level. This knowledge gap largely persists due to the lack of statistical data on species-specific interprovincial agricultural trade. Additionally, methodological challenges in accurately quantifying NH_3 emission transfers embodied in agricultural trade, stemming from inherent limitations of MRIO models, further contribute to this knowledge gap. MRIO models have been a frequently employed approach for simulating emission transfers through interregional trade (Ma *et al* 2021, Liu *et al* 2023, Ju *et al* 2024, Pan *et al* 2024). However, MRIO model applications to quantify the flows of embodied emission often provide limited insights when accounting specifically for individual agricultural products, which has prevented researchers from accounting for the composition of traded products when quantifying the NH_3 emission transfers. Limited by MRIO models, previous research commonly applied average NH_3 emission intensities to estimate emission transfers (Ma *et al* 2021), disregarding substantial provincial variations in the composition of traded products, which introduces significant uncertainties in the quantification of NH_3 emission transfers. Additionally, spatial distribution differences among crop and livestock species were often overlooked in previous research, which commonly assumed a uniform trade-related fraction of NH_3 emissions (Lin *et al* 2014, Zhang *et al* 2017, Lenzen *et al* 2018, Ma *et al* 2021). Consequently, results derived from MRIO models exhibit considerable uncertainties in both the total volume and spatial distribution of trade-related NH_3 emissions.

Compared to MRIO models, linear programming (LP) models offer advantages for simulating detailed interprovincial trade of individual agricultural products (Wang *et al* 2019a, Dalin *et al* 2014), allowing us to incorporate these previously overlooked factors into our research. This method enables more accurate quantification of NH_3 emission transfers and deepens our understanding of NH_3 emission transfers associated with specific agricultural products. Reduced uncertainty in the spatial patterns of agricultural trade-related NH_3 emissions improved the accuracy of our simulations of $PM_{2.5}$ pollution attributable to these emissions, better reflecting real-world conditions. Additionally, this advantage enables more precise understanding of how agricultural trade influences health burden across regions.

Here, we employ a LP model to simulate interprovincial trade patterns of 26 agricultural products in China and integrate these patterns with a high-resolution NH_3 emission inventory to quantify the embodied NH_3 emission transfer amounts of different agricultural products and their spatial distribution characteristics. Subsequently, we integrate the Goddard Earth Observing System Chemical Transport Model (GEOS-Chem) with the global exposure mortality model (GEMM) to explore the spatial differences in contribution of trade-related NH_3 emissions to $PM_{2.5}$ concentrations and associated premature mortality, while also analyzing the regional differences in the sensitivity of premature deaths to trade-related NH_3 emissions and its influencing factors. Finally, we characterize the health burden transfers embedded within China's interprovincial agricultural trade networks. This study provides critical insights into cross-provincial environmental impacts of agricultural trade in China, thereby informing the development of NH_3 emission reduction policies that promote environmental equity.

2. Methods

2.1. NH3 emission inventory

To obtain the NH_3 emissions per unit yield of agricultural products, we established a 2019 NH_3 emission inventory for mainland China with a $5' \times 5'$ resolution. The gridded NH_3 emissions in 2019 were calculated based on Li *et al* (Li *et al* 2021, 2024). A total of 50 sources were considered, including livestock waste, fertilizer application, synthetic ammonia, transportation, and biomass burning. The gridded NH_3 emissions were calculated using equation (1):

$$E_{NH_3} = \sum_i \sum_j \sum_k A_{i,j,k} \times EF_{i,j,k} \quad (1)$$

where i, j, and k represent the specific grid cell, source type, and month, respectively. A denotes the activity level, and EF represents the corresponding emission factor. The 2019 planted cropland area and animal population data were obtained from the National Bureau of Statistics of China (NBS 2020). The 2019 fertilizer application rates per unit area of farmland were sourced from the China Agricultural Cost–Benefit Information Compilation (NDRC 2020). The NH_3 emissions inventory established here improved on previous EF estimates of livestock waste and fertilizer application by considering the effects of soil properties, fertilizer types, temperature, and precipitation (Zhang *et al* 2018, Li *et al* 2021). The dates and times of fertilizer application were also comprehensively accounted for improving the corresponding estimation of monthly NH_3 emission distributions.

2.2. NH3 emission transfer embodied in interprovincial agriculture trade

In our study, we simulate the interprovincial trade flow of agricultural products using a LP optimization procedure that follows the CHINAGRO model framework. CHINAGRO is modeled based on the principle of transportation cost minimization and has been previously used to simulate interregional agricultural trade in China (Fischer *et al* 2007). Herein, the trade flow was obtained based on several hypotheses. First, to simplify the model, this study does not consider the influence of international trade on China's interprovincial agricultural product trade, which means the total supply (S) of traded agricultural products was equal to the total demand (D). This assumption is based on China's high agricultural self-sufficiency rate, with major NH_3-emitting agricultural products including rice, wheat, maize, vegetables, fruits, beef, lamb, pork, poultry, mutton, and eggs achieving self-sufficiency rates of 93%–100% (Huang and Xie 2022, Wang *et al* 2024). Second, it is assumed that agricultural products can flow between provinces through three transportation modes: railway, highway, and waterway. This study considered 26 agricultural products: early season rice, second rice, single-cropping rice, semilate rice, wheat, maize, soybean, potato, groundnut, rapeseed, cotton, sugarcane, sugar beet, tobacco, vegetables, apple, pear, orange, pork, beef, mutton, poultry, eggs, milk and rabbit. For a given agricultural product, the flow volume from province i to j equals the sum of flow volumes through all three transportation modes, as shown in equation (2):

$$T_{i,j,k} = T_{i,j,k,t} + T_{i,j,k,r} + T_{i,j,k,w} \quad (2)$$

where $T_{i,j,k}$ represents the total volume of agricultural products k exported from province i to j. $T_{i,j,k,t}$, $T_{i,j,k,r}$, and $T_{i,j,k,w}$ represent the transportation volume of agricultural products k from province i to j by railway, highway, and waterway, respectively. We calculated the interprovincial agriculture trade flow by minimizing the total transportation cost of trade for each product, as shown in equation (3):

$$\begin{cases} \min \sum_{i=1}^{31} \sum_{j=1}^{31} C_{i,j,t} \times T_{i,j,k,t} + C_{i,j,r} \times T_{i,j,k,r} + C_{i,j,w} \\ \quad \times T_{i,j,k,w} \\ s.t. \sum_{i=1}^{31} T_{i,j,k,t} + T_{i,j,k,r} + T_{i,j,k,w} = D_{j,k} \\ \sum_{j=1}^{31} T_{i,j,k,t} + T_{i,j,k,r} + T_{i,j,k,w} \le S_{i,k} \end{cases} \quad (3)$$

where $C_{i,j,t}$, $C_{i,j,r}$, and $C_{i,j,w}$ represent the unit weight transportation costs by railway, highway, and waterway from provinces i to j, respectively. $D_{j,k}$ represents the demand for agricultural product k in province j; $S_{i,k}$ represents the production supply of agricultural product k in province i.

The interprovincial NH_3 transfer matrix for agriculture trade is obtained by summing the NH_3 transfer matrices of all agricultural product varieties, as shown in equations (4) and (5):

$$A = \sum_k A_k \quad (4)$$

$$A_k = \begin{pmatrix} 0 & VAF_{1,2,k} & \cdots & VAF_{1,31,k} \\ VAF_{2,1,k} & 0 & \ldots & VAF_{2,31,k} \\ \vdots & \vdots & \vdots & \vdots \\ VAF_{31,1,k} & VAF_{31,2,k} & \ldots & 0 \end{pmatrix} \quad (5)$$

where A represents the interprovincial NH_3 transfer matrix for agricultural trade, A_k represents the NH_3 transfer matrix for agricultural product k. $VAF_{i,j,k}$ denotes the NH_3 emissions transferred from province i to j, which is the product of agricultural product flow volume and NH_3 emissions per unit of agricultural product, as shown in equation (6):

$$VAF_{i,j,k} = T_{i,j,k} \times \frac{E_{i,k}}{P_{i,k}} \quad (6)$$

where $E_{i,k}$ represents the NH_3 emissions from agricultural product k in province i, $P_{i,k}$ represents the production of agricultural product k in province i.

2.3. Air quality simulations and assessment of health impacts

Simulations of NH_3, $PM_{2.5}$, and their associated species were performed using the nested version of GEOS-Chem global CTM *v*.13.4.1 at 0.5° × 0.625° resolution (see text S1). The attributable premature mortality rates from $PM_{2.5}$ exposure were then quantified using the newly developed GEMM (Burnett *et al* 2018, Guo *et al* 2020, Geng *et al* 2021) (see text S2). Here the impacts due to the four leading causes of death: chronic obstructive pulmonary disease, lung cancer, ischemic heart disease, and stroke are considered. The baseline mortality rates and their 95% confidence intervals of these diseases in each age group were obtained from the global burden of disease (GBD) 2019.

2.4. Health burden transfer embodied in interprovincial agriculture trade

Here, we calculated the health burden transfer (numbers of premature deaths) embodied in interprovincial agriculture trade base on an assumption that the contribution of one source to the disease burden of $PM_{2.5}$ is directly proportional to its share of the total export-related NH_3 emissions for each province, as shown in equation (7):

$$\mathrm{Mortfloat}_{p,q} = \mathrm{Mort}_{p,\mathrm{trade}} \times \frac{VAF_{p,q}}{\sum_{p=1}^{31} VAF_{p,q}} \qquad (7)$$

where $\mathrm{Mort}_{p,\mathrm{trade}}$ represents export-related mortalities in province p. $Mortfloat_{p,q}$ represents the health burden flow from province p to q. $VAF_{p,q}$ represents the NH_3 emissions transferred from province i to j.

3. Results

3.1. NH3 emission transfer embodied in interprovincial agriculture trade

We categorize China into seven distinct geographical regions: North China (NC), Northeast China (NEC), East China (EC), Central China (CC), South China (SC), Southwest China (SWC), and Northwest China (NWC) (table S1). To quantify NH_3 emission transfer embodied in interprovincial agriculture trade, we simulated the interprovincial trade patterns of 26 agricultural products in China (see text S3 for details). In 2019, the total volume of interregional agricultural trade was 622.1 Mt, which accounted for 35.1% of total agricultural production in China. We estimate domestic grain circulation at 443.3 Mt, which shows high consistency with other studies (Zuo *et al* 2023) and is generally consistent with the official data of 576.0 Mt reported by SINOGRAIN (China's largest agricultural reserve group) (SINOGRAIN 2020).

We established a 2019 NH_3 emission inventory for mainland China to obtain NH_3 emission intensity per unit yield of agricultural products (figure S4). NH_3 emission intensity varied substantially across agricultural products (figure S5). Livestock products exhibited significantly higher emission intensity (30.0 kg t^{-1}) compared to crop products (2.7 kg t^{-1}). Among crops, sugarcane exhibited the lowest NH_3 emission intensity (0.3 kg t^{-1}) and cotton the highest (35.3 kg t^{-1}), while in the livestock sector, poultry meat (6.5 kg t^{-1}) and beef (296.2 kg t^{-1}) represented the lowest and highest intensities, respectively. Notable regional variations in NH_3 emission intensity were observed for identical agricultural products (figure S5). For instance, the emission intensity of wheat ranged from 1.9 kg t^{-1}in Heilongjiang to 14.3 kg t^{-1} in Inner Mongolia, primarily due to substantial regional differences in fertilizer application rates, with urea application for wheat cultivation in Inner Mongolia (659.35 kg hm^{-2}) far exceeding that in Heilongjiang (71.74 kg hm^{-2}) (NDRC 2020). The emission intensity of beef varied from 98.6 kg t^{-1} in Hebei to 854.0 kg t^{-1} in Qinghai, mainly attributed to significant regional disparities in livestock farming intensification, with the intensification ratio of beef cattle farming in Hebei (21%) substantially higher than in Qinghai (5%) (Hu 2020).

The importation of agricultural products resulted in the transfer of production-related NH_3 emissions from importing to exporting regions. The total NH_3 emissions embodied in interregional trade were 2.94 Tg in 2019, which was 28.1% of China's agricultural emissions. Interregional NH_3 emission transfers revealed a distinct flow from wealthier eastern and southern China to northern and central China (figure 1). EC (0.86 Tg) and SC (0.84 Tg) emerged as the primary NH_3-emission-exporting regions, while NEC (0.55 Tg) and NWC (0.50 Tg) were the main NH_3-emission-importing regions. Here, a province 'importing' NH_3 emissions from other provinces refers to the transfer of NH_3 emissions associated with the production of these outflowed agricultural products to that province when the province exports agricultural products to other provinces; while 'exporting' NH_3 emissions represents the opposite, indicating the outward transfer of NH_3 emissions when agricultural products flow into the province. Among these regions, SC exhibited the largest net emissions export (0.73 Tg), while NEC showed the largest net import (0.41 Tg). Provincial analysis identified Guangdong as the largest net emission exporter (0.62 Tg) and Heilongjiang as the largest net importer (0.27 Tg) (figure 2). The most substantial interregional flow of NH_3 emissions occurred from EC to NEC (0.35 Tg). Notably, the spatial distribution of NH_3 emission transfers exhibited marked divergence from agricultural trade patterns, primarily driven by regional heterogeneity in traded product composition. For instance, SC, while

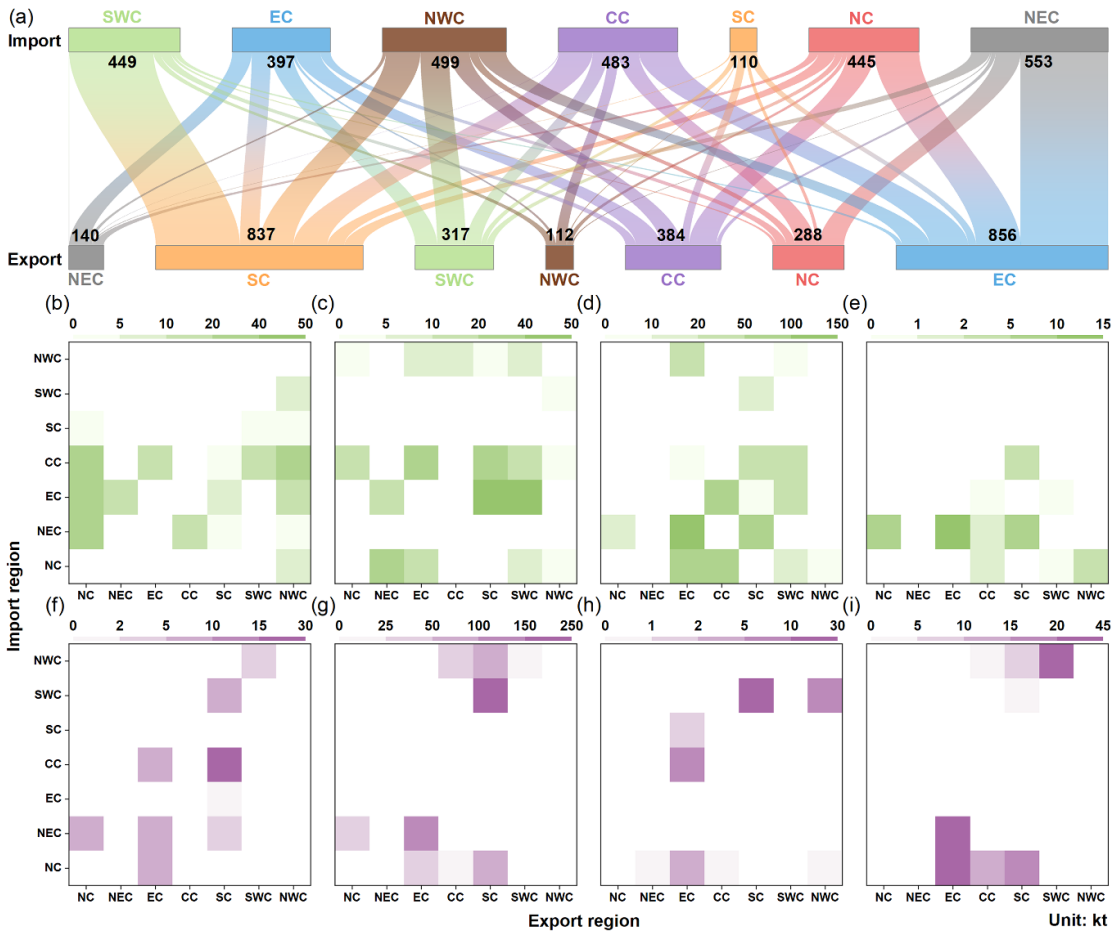

Figure 1. NH_3 emission transfers embodied in interregional agricultural trade. (a), Total interregional NH_3 emission transfers. Interregional NH_3 transfers for rice (b), wheat (c), corn (d), soybeans (e), pork (f), beef (g), lamb (h), and dairy products (i). Abbreviations for regions: NEC (Northeast China), CC (Central China), SC (South China), NWC (Northwest China), NC (North China), SWC (Southwest China), and EC (East China).

being the greatest net NH_3 emission exporter, shows the least net agricultural product imports (0.04 Mt). This disparity is attributed to the significantly higher proportion of livestock products in SC's imports (12.01%) compared to its exports (0.05%), with livestock products generally exhibiting higher emission intensity.

Interregional crop trade resulted in NH_3 transfers of 1932.5 kt, accounting for 43.3% of total crop-related NH_3 emissions (figure S5(a)). The strongest net outflow of crop-related NH_3 emissions occurred in SC (238.7 kt), which was mainly flowed to NEC (64.1 kt) and CC (62.8 kt). By contrast, NWC experienced the strongest net inflow (197.1 kt), predominantly originating from EC (100.2 kt). Among crop products, maize trade generated the largest NH_3 emission transfers (562.0 kt), representing 29.1% of total crop-trade-related NH_3 emissions. The most significant transfer pathway was observed from EC to NEC (131.8 kt), a major maize-producing region. The total volume of NH_3 emissions flow caused by interregional livestock trade was 1003.0 kt, accounting for 16.8% of total livestock-related NH_3 emissions (figure S5(b)). SC demonstrated the largest net outflow of livestock-related NH_3 emissions (488.8 kt), while NEC showed the largest net inflow (234.6 kt). SC's emission outflow was primarily directed to SWC (268.7 kt), while NEC's emission inflow mainly originated from EC (185.1 kt). Among livestock products, beef trade dominated the livestock-related NH_3 emission transfer (630.8 kt), accounting for 62.9% of the total. The transfer pathway from SC to SWC exhibited the highest volume, with transfers totaling 229.4 kt.

3.2. Impacts of trade-related NH3 emissions on PM2.5 concentrations and human health

In 2019, trade-related NH_3 emissions contributed 2.6 $\mu g\ m^{-3}$ to annual $PM_{2.5}$ concentrations across mainland China, accounting for 16.1% of total $PM_{2.5}$ levels. The spatial distribution of these contributions exhibited significant heterogeneity (figure 3(a)). Elevated $PM_{2.5}$ concentrations were identified in CC (9.0 $\mu g\ m^{-3}$), and EC (7.5 $\mu g\ m^{-3}$), driven by their notably high trade-related NH_3 emission

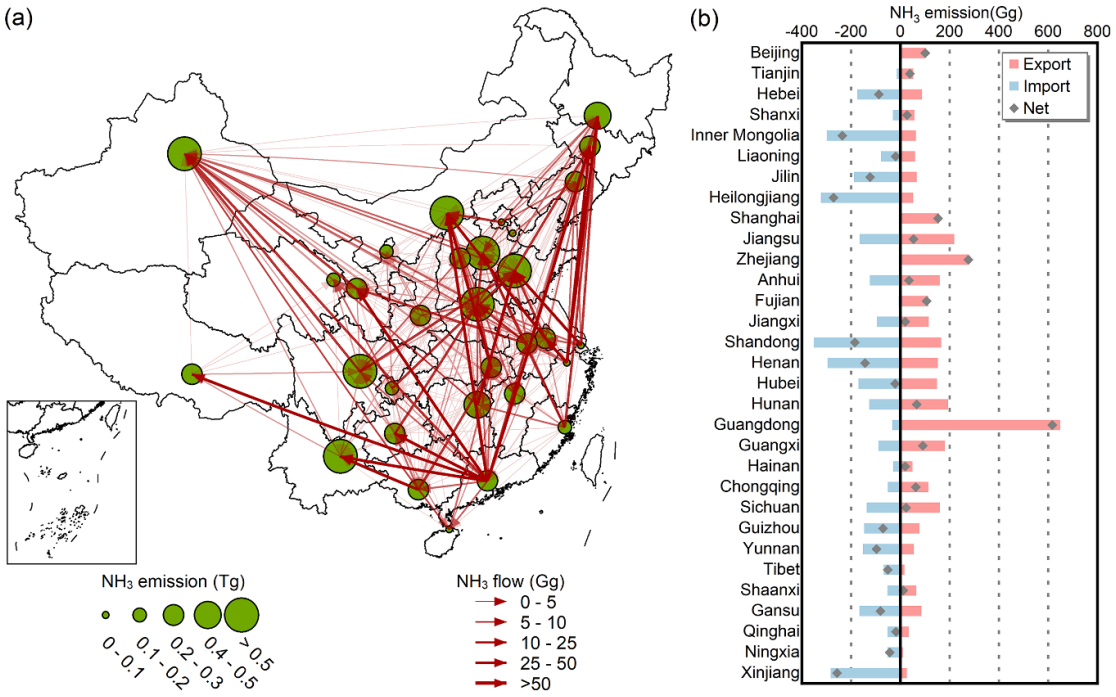

Figure 2. Interprovincial transfers of agricultural NH_3 emissions. (a) The spatial pattern of net NH_3 emission transfers embodied in interprovincial agricultural trade. The width of line represents the net flow volume of NH_3 emission, and arrows indicate transfer direction. (b) Sum of NH_3 emission transferred. Positive numbers indicate exports, while negative numbers represent imports.

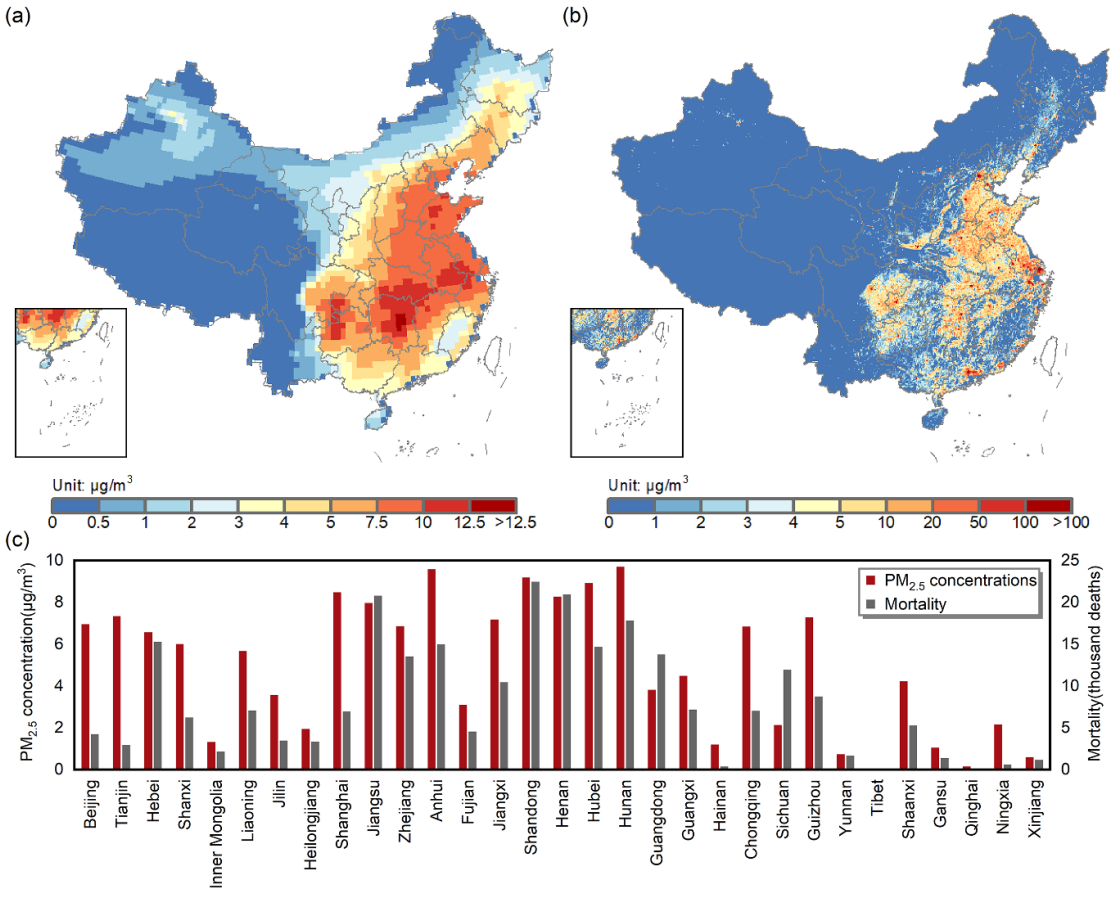

Figure 3. Impacts of trade-related NH_3 emissions on $PM_{2.5}$ concentrations and human health. (a) $PM_{2.5}$ concentrations induced by export-related NH_3 emissions in 2019. (b) Attributable premature mortality due to export-related NH_3 emissions. (c) Provincial contributions of export-related NH_3 emissions to average $PM_{2.5}$ concentrations and premature mortality.

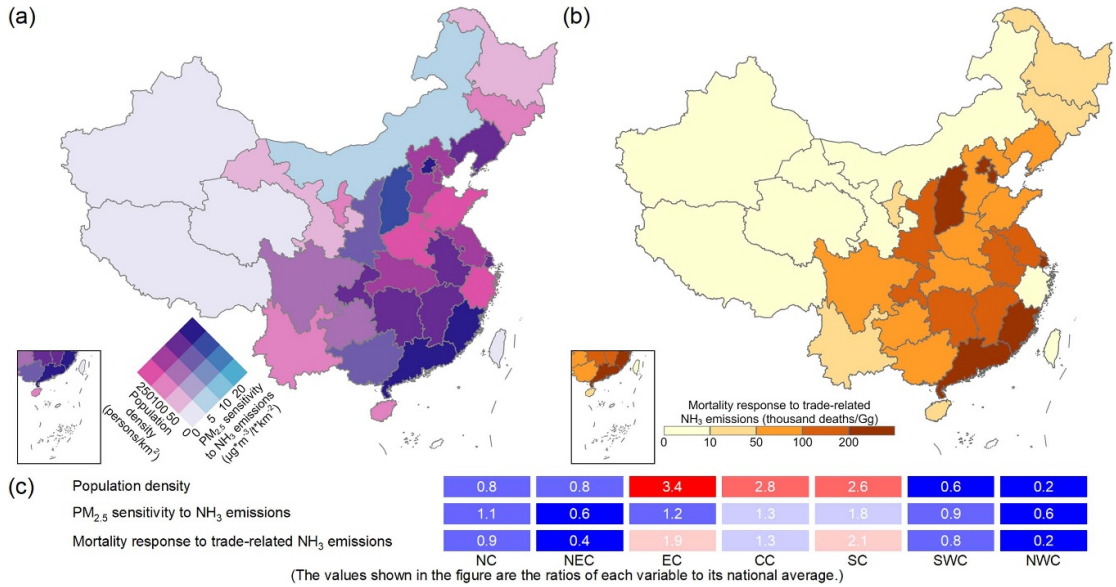

Figure 4. Spatial differences in population density, $PM_{2.5}$ sensitivity to NH_3 emissions, and mortality response to trade-related NH_3 emissions. (a) Provincial population density and $PM_{2.5}$ sensitivity to NH_3 emissions. (b) Provincial mortality response to trade-related NH_3 emissions. (c) Regional population density, $PM_{2.5}$ sensitivity to NH_3 emissions, and mortality response to trade-related NH_3 emissions.

densities (1.15 t km^{-2} and 1.12 t km^{-2}, respectively), which substantially exceeded the national average (0.44 t km^{-2}). At the provincial level, Hunan (9.7 μg m^{-3}), Anhui (9.6 μg m^{-3}), and Shandong (9.2 μg m^{-3}) demonstrated the most substantial contributions to $PM_{2.5}$ concentrations from trade-related NH_3 emissions (figure 3(c)). The high trade-related NH_3 emission densities in Central and Eastern China are driven by industrial structural transformations that have occurred over the past four decades. With rapid industrialization in southeastern coastal regions, extensive agricultural land has been converted to industrial use while agricultural product demand has increased rapidly, making these regions highly dependent on agricultural supply from other regions. In Guangdong and Guangxi, grain self-sufficiency declined from nearly 70% in 1990 to less than 40% in 2015 (Zuo *et al* 2023). Due to water resource constraints, northwestern regions lack the capacity for large-scale agricultural development. In contrast, Central and Eastern China, benefiting from favorable natural conditions, modern agricultural technology adoption, and policy support, have emerged as primary agricultural suppliers.

The spatial distribution of trade-related NH_3 emissions did not directly correspond to their impact on $PM_{2.5}$ concentrations due to regional variations in $PM_{2.5}$ sensitivity to NH_3 emissions (μg m^{-3} per kg NH_3 m^{-2} yr^{-1}) (figure 4). SC's trade-related NH_3 emission density was only 29% of that observed in CC, yet its contribution to $PM_{2.5}$ concentrations reached 44% of CC's levels, reflecting SC's highest $PM_{2.5}$ sensitivity to NH_3 emissions, double the average across regions. Conversely, NEC, a major grain-exporting region, despite having trade-related NH_3 emission density at 74% of CC's level, contributed only 33% to $PM_{2.5}$ concentrations relative to CC, attributable to NEC's lowest $PM_{2.5}$ sensitivity to NH_3 emissions (0.59 times the regional average).

The estimated premature mortality attributable to $PM_{2.5}$ exposure in 2019 was 1549 778 (95% CI 1229 480–1736 806) deaths, with 252 016 (95% CI 199 918–282 420) (16.3%) deaths associated with agricultural trade-related NH_3 emissions. The spatial patterns of trade-related $PM_{2.5}$ concentrations closely aligned with their impacts on premature mortality (figure 3(b)), as regions with elevated $PM_{2.5}$ concentrations from trade-related NH_3 emissions coincided with areas of high population density. EC and CC exhibited the highest trade-related mortality, accounting for 93 952 (95% CI 74 519–105 202) and 53 503 (95% CI 42 424–59 936) premature deaths, respectively. At the provincial level, Shandong (22 494 (95% CI 17 836–25 199)), Henan (20 976 (95% CI 16 632–23 497)), and Jiangsu (20 835 (95% CI 16 523–23 320)) recorded the highest numbers of trade-related premature deaths. The spatial distribution of trade-related NH_3 emissions showed substantial divergence from their contribution to premature mortality (figure 3), primarily due to regional variations in population density and $PM_{2.5}$ sensitivity to

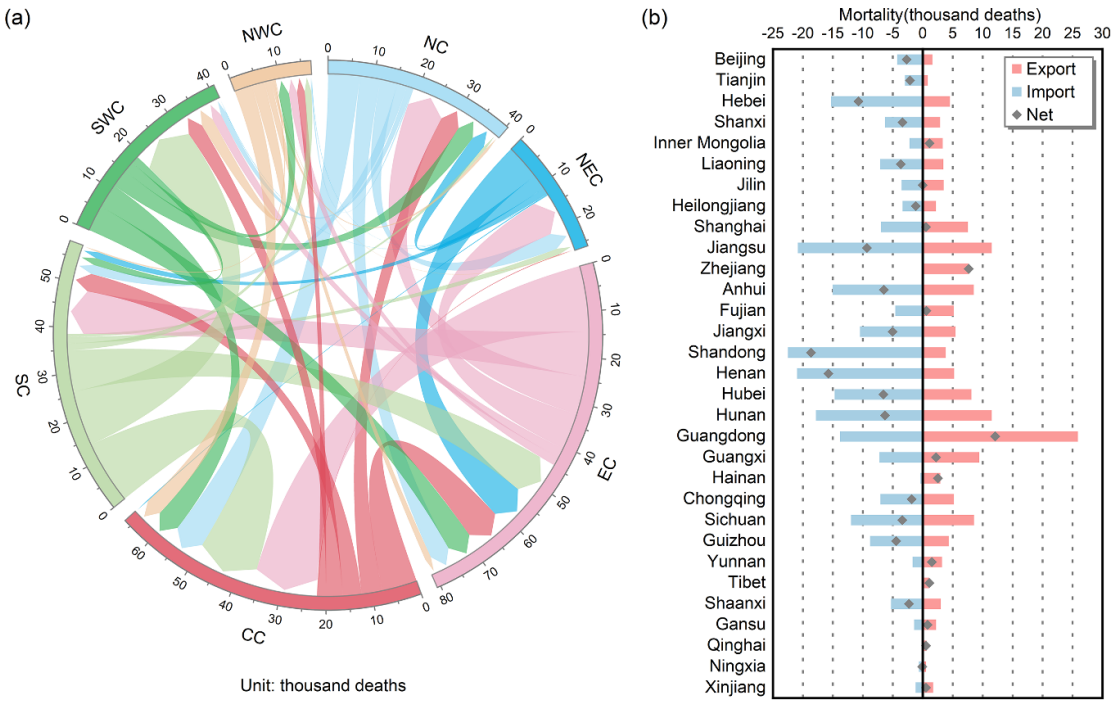

Figure 5. Health burden transfers (number of premature deaths) through agricultural trade. (a) Interregional transfers of health burden. The width of ribbons denotes the volume of health burden flow. The connection between regions indicates the health burden transfer and the color of ribbons in line with the exporter. (b) Sum of health burden transfers at provincial level. Positive numbers indicate exports, while negative numbers represent imports. Abbreviations for regions: NEC (Northeast China), CC (Central China), SC (South China), NWC (Northwest China), NC (North China), SWC (Southwest China), and EC (East China).

NH_3 emissions. For instance, NEC, while accounting for 15.7% of national trade-related NH_3 emissions, contributed only 5.5% to national trade-related premature mortality. This discrepancy stemmed from its lower mortality response to trade-related NH_3 emissions (24 deaths Gg^{-1} compared to the national average of 67 deaths Gg^{-1}), resulting from the region's lower population density, lower baseline $PM_{2.5}$ concentrations, and reduced $PM_{2.5}$ sensitivity to NH_3 emissions.

The spatial disparities between trade-related NH_3 emissions and premature mortality reflect the complex relationships between agricultural trade and its impact on health burden. We analyzed spatial differences in population density, $PM_{2.5}$ sensitivity to NH_3 emissions, and mortality response to trade-related NH_3 emissions (figure 4). For convenience, we normalized these regional values by dividing each variable in each region by its national average. Mortality responses to trade-related NH_3 emissions exceeded national averages in SC, EC, CC, and NC, while remaining below average in SWC, NEC, and NWC. The high value in SC (2.1) was primarily attributed to higher population density (2.6) and $PM_{2.5}$ sensitivity to NH_3 emissions (1.8). The low value in NEC (0.4) resulted mainly from lower $PM_{2.5}$ sensitivity to NH_3 emissions (0.6). The contrasting population densities between NEC and SC reflect the spatial difference in economic development, where rapid economic development in eastern and southern coastal provinces has driven population migration from the predominantly agricultural NEC. The significant differences in $PM_{2.5}$ sensitivity to NH_3 emissions between SC and NEC likely stem from distinct atmospheric NH_3 saturation states, with SC being NH_3-limited and NEC being NH_3-rich. Notably, SC and NEC are the largest net exporter and importer of NH_3 emissions respectively, suggesting that agricultural trade can prevent additional premature deaths by redistributing emissions from densely populated, NH_3-limited regions to sparsely populated, NH_3-rich regions. These findings suggest that optimizing trade structures based on regional population density and atmospheric NH_3 saturation could mitigate health burden from food system in future agricultural and environmental policies.

3.3. Health burden transfer embodied in interprovincial agriculture trade

To track the origins of health impacts, we identified the transfer network of premature deaths associated with agricultural trade (figure 5(a)). Interregional agricultural trade resulted in the transfer of 165 thousand premature deaths, accounting for 10.7% of total $PM_{2.5}$-related premature mortality. EC (44.6 thousand deaths) and SC (38.5 thousand deaths) emerged as the primary mortality-exporting regions, collectively accounting for 50.3% of total transfers, while CC (44.6 thousand deaths) and EC (36.2 thousand deaths) were the main importing

regions, representing 48.9% of total transfers. EC, as the largest mortality-exporting region, primarily transferred premature deaths to CC (14.3 thousand deaths) and SC (9.9 thousand deaths). CC, as the largest recipient of premature deaths, mainly received transported mortality from EC (14.3 thousand deaths) and SC (13.8 thousand deaths).

The current trade structure has adverse effects on the public health of net-importing regions (CC, SWC, NC, and NEC), which collectively received a net inflow of 28.8 thousand premature deaths, while net-exporting regions (SC, EC, and NWC) demonstrated health benefits. At the provincial level, net-exporting provinces transferred 31 228 premature deaths to net-importing provinces (figure 5(b)). CC showed the largest net import of premature deaths (22.6 thousand), while SC exhibited the largest net export (18.9 thousand deaths). At the provincial level, Shandong recorded the highest net import (18.6 thousand deaths), while Guangdong demonstrated the highest net export (12.1 thousand deaths).

The spatial distribution of health burden transfers diverged significantly from NH_3 emission transfers, primarily due to regional variations in mortality response to trade-related NH_3 emissions. For example, while EC transfers similar numbers of premature mortality to NEC and SC (4.79% and 5.98% of total mortality transfers, respectively), its NH_3 emission transfers to these regions differ substantially (12.58% and 1.10% of total NH_3 transfers, respectively). This discrepancy stems from regional differences in mortality response rates: NEC shows a notably lower response (24 deaths Gg^{-1}) compared to the national average (67 deaths Gg^{-1}), while SC exhibits a significantly higher response (141 deaths Gg^{-1}). At the provincial level, these spatial disparities became even more pronounced, with over half of provinces showing opposite patterns in their net balance of health burden and NH_3 emission transfers (figure 5(b)). A notable example is Inner Mongolia, which, despite being a primary net importer of NH_3 emissions, emerged as a net exporter of health burden, attributable to its exceptionally low mortality response to trade-related NH_3 emissions (merely 1/9 of the national average).

4. Conclusions

The expansion of agricultural trade networks has intensified the transfer of NH_3 emissions and its impacts on air quality and public health, factors that will be increasingly critical for sustainable agricultural development in China. Previous research on agricultural emissions was based solely on production while overlooking the significant role of agricultural trade. This study achieved more accurate estimations of the impact of agricultural trade on health burden by simulating trade in individual crop and livestock product varieties and considering spatial distribution differences among crop and livestock species. It provides, for the first time, detailed geographical insights into interprovincial NH_3 emission transfers and associated health impacts across China.

This study provides a comprehensive analysis of NH_3 emission transfers through interprovincial agricultural trade in China. Interregional agricultural trade reached 622.1 Mt in 2019, accounting for 35.05% of total production. Agricultural trade has significantly reshaped the spatial distribution of NH_3 emissions. Approximately 28.1% of agricultural NH_3 emissions (2.94 Tg) are trade-related, which primarily flowed from eastern and southern China to northern and central China. Trade-related NH_3 emissions contribute 2.6 $\mu g\ m^{-3}$ to annual $PM_{2.5}$ concentrations and cause 252 016 premature deaths in mainland China, accounting for over 16% of both impacts. The highest contributions were observed in CC (9.0 $\mu g\ m^{-3}$, 54 thousand deaths) and EC (7.5 $\mu g\ m^{-3}$, 94 thousand deaths). Mortality response to trade-related NH_3 emissions showed distinct spatial heterogeneity across China, ranging from 14 deaths Gg^{-1} in NWC to 141 deaths Gg^{-1} in SC, driven by regional variations in population density and $PM_{2.5}$ sensitivity to NH_3 emissions. The mortality response in SC is six times that of NEC. This is primarily attributed to SC's population density and $PM_{2.5}$ sensitivity to NH_3 emissions both exceeding those of NEC by threefold. The substantial difference in $PM_{2.5}$ sensitivity to NH_3 emissions between SC and NEC results from differences in atmospheric NH_3 saturation. This finding indicates that in future agricultural and environmental management policy-making, optimizing trade structures to redistribute NH_3 emissions from densely populated, NH_3-limited regions to sparsely populated, NH_3-rich regions could mitigate the health burden from food systems.

Agricultural trade reshapes the spatial distribution of health burdens by transferring NH_3 emissions between regions with significant differences in population density and $PM_{2.5}$ sensitivity to NH_3 emissions. Notably, CC, SWC, NC, and NEC experienced a net inflow of 28 776 premature deaths due to agricultural trade. We also found that the spatial heterogeneity in mortality response to trade-related NH_3 emissions creates a disconnect between the flow pattern of health burden and NH_3 emission, with over half of provinces showing opposite patterns in their net balance of health burden and NH_3 emission transfers. Although agricultural trade ensures food security in well-developed and densely populated regions, it is essential to consider the potential impacts of such trade on environmental equity across China's diverse regional contexts. On the basis of this research, regional compensation mechanisms, such as food taxes to subsidize production regions, and NH_3 emission quota allocation based on the

proportion of agricultural trade benefits and health burden inflows are recommended to promote environmental equity and balance consumer demand for food security with producer requirements for NH_3 emission reduction (Zheng *et al* 2024). Some limitations exist in this study, i.e. uncertainties in agricultural trade simulation and trade-related NH_3 emissions. For agricultural trade simulation, the impact of international trade on China's interprovincial agricultural trade has not been considered. However, this limitation likely has minimal impact on our results given China's high agricultural self-sufficiency rate (Ito and Ni 2013, Huang and Xie 2022, Wang *et al* 2024). Additionally, consistent with previous studies, our LP approach does not account for non-market factors influencing trade flows due to data limitations and model simplification requirements (Wang *et al* 2019a, Zuo *et al* 2023, Luo *et al* 2025). Future work could enhance the accuracy of simulations by incorporating those factors into the LP model. For trade-related NH_3 emissions, the provincial-scale agricultural trade simulation limits our ability to assess the impact of intra-provincial variations on trade-related NH_3 emissions. Future research should extend the LP model to the city level and explore the temporal evolution of the flow pattern of agricultural trade-related NH_3 emissions.

Data availability statement

All data that support the findings of this study are included within the article (and any supplementary files).

Acknowledgment

The work was financially supported by the National Natural Science Foundation of China (Grant Nos. 42361144876 and 42377393). We express our gratitude to the developers of GEOS-Chem for openly sharing their source code. We acknowledge the Multi-resolution Emission Inventory model team (MEIC, China) for making their data publicly available.

Conflict of interest

The authors declare that they have no known competing financial interests of personal relationships that could have appeared to influence the work reported in this paper.

ORCID iDs

Baojie Li 0000-0002-3747-6534
Qing Zhu 0000-0002-5798-3883
Yan Li 0000-0003-0340-6033
Hong Liao 0000-0001-6628-1798

References

Ali T, Huang J, Wang J and Xie W 2017 Global footprints of water and land resources through China's food trade *Glob. Food Secur.* **12** 139–45

Bai Z, Winiwarter W, Klimont Z, Velthof G, Misselbrook T, Zhao Z, Jin X, Oenema O, Hu C and Ma L 2019 *Further Improvement of Air Quality in China Needs Clear Ammonia Mitigation Target* (ACS Publications)

Burnett R T, Pope C A III, Ezzati M, Olives C, Lim S S, Mehta S, Shin H H, Singh G, Hubbell B and Brauer M 2014 An integrated risk function for estimating the global burden of disease attributable to ambient fine particulate matter exposure *Environ. Health Perspect.* **122** 397–403

Burnett R, Chen H, Szyszkowicz M, Fann N, Hubbell B, Pope C A III, Apte J S, Brauer M, Cohen A and Weichenthal S 2018 Global estimates of mortality associated with long-term exposure to outdoor fine particulate matter. *Proc. Natl Acad. Sci.* **115** 9592–7

Chen K, Huang T, Zhang X, Liu X, Jian X, Zhugu R, Wang L, Tao S, Liu J and Gao H 2022 Drivers of global methane emissions embodied in international beef trade *Environ. Sci. Technol.* **56** 11256–65

Dalin C, Hanasaki N, Qiu H, Mauzerall D L and Rodriguez-Iturbe I 2014 Water resources transfers through Chinese interprovincial and foreign food trade *Proc. Natl Acad. Sci.* **111** 9774–9

Feng K, Davis S J, Sun L, Li X, Guan D, Liu W, Liu Z and Hubacek K 2013 Outsourcing CO_2 within china *Proc. Natl Acad. Sci.* **110** 11654–9

Fischer G, Huang J, Keyzer M A, Qiu H, Sun L and van Veen W C M 2007 *China's agricultural prospects and challenges: Report on scenario simulations until 2030 with the Chinagro welfare model covering national, regional and county level*

Fu X, Wang S, Xing J, Zhang X, Wang T and Hao J 2017 Increasing ammonia concentrations reduce the effectiveness of particle pollution control achieved via SO_2 and NO_X emissions reduction in east China *Environ. Sci. Technol. Lett.* **4** 221–7

Geng G, Zheng Y, Zhang Q, Xue T, Zhao H, Tong D, Zheng B, Li M, Liu F and Hong C 2021 Drivers of $PM_{2.5}$ air pollution deaths in China 2002–2017 *Nat. Geosci.* **14** 645–50

Gu B, Zhang L, Van Dingenen R, Vieno M, Van Grinsven H J, Zhang X, Zhang S, Chen Y, Wang S and Ren C 2021 Abating ammonia is more cost-effective than nitrogen oxides for mitigating $PM_{2.5}$ air pollution *Science* **374** 758–62

Guo Y, Chen Y, Searchinger T D, Zhou M, Pan D, Yang J, Wu L, Cui Z, Zhang W and Zhang F 2020 Air quality, nitrogen use efficiency and food security in China are improved by cost-effective agricultural nitrogen management *Nat. Food* **1** 648–58

Guo Y, Zhang L, Winiwarter W, van Grinsven H J, Wang X, Li K, Pan D, Liu Z and Gu B 2024 Ambitious nitrogen abatement is required to mitigate future global $PM_{2.5}$ air pollution toward the world health organization targets *One Earth* **7** 1600–13

Hu L 2020 *China Animal Husbandry and Veterinary Yearbook* (China Agriculture Press)

Huang J and Xie W 2022 China's future food supply and demand: prospects and policies *Front. Sci. Technol. Eng. Manag.* **41** 17–25

Huang X, Song Y, Li M, Li J, Huo Q, Cai X, Zhu T, Hu M and Zhang H 2012 A high-resolution ammonia emission inventory in China *Glob. Biogeochem. Cycles* **26**

Ito J and Ni J 2013 Capital deepening, land use policy, and self-sufficiency in China's grain sector *China Econ. Rev.* **24** 95–107

Ju H, Zeng G and Zhang S 2024 Inter-provincial flow and influencing factors of agricultural carbon footprint in China and its policy implication *Environ. Impact Assess. Rev.* **105** 107419

Lenzen M, Sun Y-Y, Faturay F, Ting Y-P, Geschke A and Malik A 2018 The carbon footprint of global tourism *Nat. Clim. Change* **8** 522–8

Li B, Chen L, Shen W, Jin J, Wang T, Wang P, Yang Y and Liao H 2021 Improved gridded ammonia emission inventory in China *Atmos. Chem. Phys.* **21** 15883–900

Li B, Liao H, Li K, Wang Y, Zhang L, Guo Y, Liu L, Li J, Jin J and Yang Y 2024 Unlocking nitrogen management potential via large-scale farming for air quality and substantial co-benefits *Natl Sci. Rev.* **11** nwae324

Lin J, Pan D, Davis S J, Zhang Q, He K, Wang C, Streets D G, Wuebbles D J and Guan D 2014 China's international trade and air pollution in the United States *Proc. Natl Acad. Sci.* **111** 1736–41

Liu G, Zhang F and Deng X 2023 Half of the greenhouse gas emissions from China's food system occur during food production *Commun. Earth Environ.* **4** 161

Liu M, Huang X, Song Y, Tang J, Cao J, Zhang X, Zhang Q, Wang S, Xu T and Kang L 2019 Ammonia emission control in China would mitigate haze pollution and nitrogen deposition, but worsen acid rain *Proc. Natl Acad. Sci.* **116** 7760–5

Liu W, Yang H, Liu Y, Kummu M, Hoekstra A Y, Liu J and Schulin R 2018 Water resources conservation and nitrogen pollution reduction under global food trade and agricultural intensification *Sci. Total Environ.* **633** 1591–601

Liu X, Yu L, Cai W, Ding Q, Hu W, Peng D, Li W, Zhou Z, Huang X and Yu C 2021 The land footprint of the global food trade: perspectives from a case study of soybeans *Land Use Policy* **111** 105764

Luo L, Xing Z, Liu Y, Liu X, Jiang L, Peng Y, Zhang H and Wang H 2025 A dataset of interprovincial food trade flows in China *Sci. Data* **12** 1–12

Ma R, Li K, Guo Y, Zhang B, Zhao X, Linder S, Guan C, Chen G, Gan Y and Meng J 2021 Mitigation potential of global ammonia emissions and related health impacts in the trade network *Nat. Commun.* **12** 6308

NBS 2020 *China Statistical Yearbook* (China Statistics Press)

NDRC 2020 *National Agricultural Product Cost Benefit Information Compilation* (China Statistics Press)

Pan H, Zheng X, Wu R, Liu X, Xiao S, Sun L, Hu T, Gao Z, Yang L and Huang C 2024 Agriculture related methane emissions embodied in China's interprovincial trade *Renew. Sustain. Energy Rev.* **189** 113850

Qiang W, Liu A, Cheng S, Kastner T and Xie G 2013 Agricultural trade and virtual land use: the case of China's crop trade *Land Use Policy* **33** 141–50

SINOGRAIN 2020 *Corporate Social Responsibility Report*

Wang S, Xing J, Jang C, Zhu Y, Fu J S and Hao J 2011 Impact assessment of ammonia emissions on inorganic aerosols in East China using response surface modeling technique *Environ. Sci. Technol.* **45** 9293–300

Wang Y, Zhu Z, Dong H, Zhang X, Wang S and Gu B 2024 Mitigation potential of methane emissions in China's livestock sector can reach one-third by 2030 at low cost *Nat. Food* **5** 603–14

Wang Z, Zhang L, Ding X and Mi Z 2019a Virtual water flow pattern of grain trade and its benefits in China *J. Clean. Prod.* **223** 445–55

Wang Z, Zhang L, Zhang Q, Wei Y-M, Wang J-W, Ding X and Mi Z 2019b Optimization of virtual water flow via grain trade within China *Ecol. Indic.* **97** 25–34

Wei W, Hao S, Yao M, Chen W, Wang S, Wang Z, Wang Y and Zhang P 2020 Unbalanced economic benefits and the electricity-related carbon emissions embodied in China's interprovincial trade *J. Environ. Manage.* **263** 110390

Wu S, Ben P, Chen D, Chen J, Tong G, Yuan Y and Xu B 2018 Virtual land, water, and carbon flow in the inter-province trade of staple crops in China *Resour. Conserv. Recycl.* **136** 179–86

Xie Y, Dai H, Dong H, Hanaoka T and Masui T 2016 Economic impacts from $PM_{2.5}$ pollution-related health effects in China: a provincial-level analysis *Environ. Sci. Technol.* **50** 4836–43

Yang B, Ke X, van Vliet J, Yu Q, Zhou T and Verburg P H 2020 Impact of cropland displacement on the potential crop production in China: a multi-scale analysis *Reg. Environ. Change* **20** 1–13

Yang Z, Mao X, Zhao X and Chen B 2012 Ecological network analysis on global virtual water trade *Environ. Sci. Technol.* **46** 1796–803

Zhan X, Adalibieke W, Cui X, Winiwarter W, Reis S, Zhang L, Bai Z, Wang Q, Huang W and Zhou F 2020 Improved estimates of ammonia emissions from global croplands *Environ. Sci. Technol.* **55** 1329–38

Zhang H, Zhang W, Lu Y, Wang Y, Shan Y, Ping L, Li H, Lee L-C, Wang T and Liang C 2023 Worsening carbon inequality embodied in trade within China *Environ. Sci. Technol.* **57** 863–73

Zhang L, Chen Y, Zhao Y, Henze D K, Zhu L, Song Y, Paulot F, Liu X, Pan Y and Lin Y 2018 Agricultural ammonia emissions in China: reconciling bottom-up and top-down estimates *Atmos. Chem. Phys.* **18** 339–55

Zhang Q, Jiang X, Tong D, Davis S J, Zhao H, Geng G, Feng T, Zheng B, Lu Z and Streets D G 2017 Transboundary health impacts of transported global air pollution and international trade *Nature* **543** 705–9

Zheng L *et al* 2024 Health burden from food systems is highly unequal across income groups *Nat. Food* **5** 251–61

Zhuo L, Mekonnen M M and Hoekstra A Y 2016 The effect of inter-annual variability of consumption, production, trade and climate on crop-related green and blue water footprints and inter-regional virtual water trade: a study for China (1978–2008) *Water Res.* **94** 73–85

Zuo C, Wen C, Clarke G, Turner A, Ke X, You L and Tang L 2023 Cropland displacement contributed 60% of the increase in carbon emissions of grain transport in China over 1990–2015 *Nat. Food* **4** 223–35